

# Low-Cost Behavioral Modeling of Antennas by Dimensionality Reduction and Domain Confinement

Slawomir Koziel<sup>1,2</sup>[0000-0002-9063-2647], Anna Pietrenko-Dabrowska<sup>2</sup>[0000-0003-2319-6782],  
and Leifur Leifsson<sup>3</sup>[0000-0001-5134-870X]

- <sup>1</sup> Engineering Optimization & Modeling Center, Department of Engineering, Reykjavik University, Menntavegur 1, 102 Reykjavik, Iceland  
koziel@ru.is
- <sup>2</sup> Faculty of Electronics Telecommunications and Informatics, Gdansk University of Technology, Narutowicza 11/12, 80-233 Gdansk, Poland  
anna.dabrowska@pg.edu.pl
- <sup>3</sup> School of Aeronautics and Astronautics, Purdue University, West Lafayette, IN 47907, USA  
leifur@purdue.edu

**Abstract.** Behavioral modeling has been rising in importance in modern antenna design. It is primarily employed to diminish the computational cost of procedures involving massive full-wave electromagnetic (EM) simulations. Cheaper alternative offer surrogate models, yet, setting up data-driven surrogates is impeded by, among others, the curse of dimensionality. This article introduces a novel approach to reduced-cost surrogate modeling of antenna structures, which focuses the modeling process on design space regions containing high-quality designs, identified by randomized pre-screening. A supplementary dimensionality reduction is applied via the spectral analysis of the random observable set. The reduction process identifies the most important directions from the standpoint of geometry parameter correlations, and spans the domain along a small subset thereof. As demonstrated, domain confinement as outlined above permits a dramatic improvement of surrogate accuracy in comparison to the state-of-the-art modeling approaches.

**Keywords:** Antenna design, surrogate modeling, behavioral modeling, dimensionality reduction, domain confinement, EM-driven design.

## 1 Introduction

Contemporary antenna design largely relies on full-wave electromagnetic (EM) simulation tools, which are indispensable to account for mutual coupling effects [1]. Parameter tuning is increasingly often performed using rigorous numerical methods [2]. Yet, the major setback of EM-driven optimization is its high computational cost, often problematic for local tuning [3], and usually unmanageable for global search [4]. An extensive research has been devoted to expediting simulation-based design. Some of techniques attempt to lower the cost of direct EM-driven optimization (adjoint sensitivities [5], restricted Jacobian updates [6]). In surrogate modeling, expensive EM simulations are replaced by fast metamodels, which may be data-driven [7] or physics-based ones [8]. The

former (kriging [9] or neural networks [10]) are significantly more popular due to their versatility and accessibility. The bottleneck of data-driven metamodels is the curse of dimensionality but also nonlinearity of high-frequency system responses. Physics-based modeling techniques (e.g., space mapping [11]) are less prone to the mentioned difficulties. Other approaches capitalize on the distinctive shape of the system responses (e.g., feature-based technology [12]). Still, constructing accurate models is impeded by the problems related to dimensionality and extensive ranges of material and geometry parameters, the surrogate should be valid for to ensure its design utility.

In [13], a performance-driven methodology has been put forward, in which the modeling process is carried out in the section of the parameter space comprising designs of high quality w.r.t. the assumed figures of interest. Volume reduction permits radical improvement of the model predictive power [14]. From computational perspective, the limitation of this method is that the surrogate model domain is outlined using pre-optimized database designs, acquisition of which incurs considerable costs. In a recent alternative [15]; however, the domain is determined using a stochastic pre-selection procedure, thus no reference designs are employed.

This article proposes an advancement over the approach of [15], where the surrogate domain defined through pre-selection is further confined by means of the spectral analysis of the observable set. The final domain is spanned by a small number of eigenvectors of the covariance matrix of the observables. The outcome is a considerably improved accuracy and scalability of the model predictive power as a function of the training data set size. At the same time, design usability of the surrogate is retained.

## 2 Domain-Confined Modeling Using Pre-Screening and Dimensionality Reduction

This section outlines the observable-based constrained modeling framework [15], being the core of our approach. Further, the inverse regression model employed for domain definition purposes is described, as well as dimensionality reduced domain.

### 2.1 Performance-Driven Modeling

Our approach capitalizes reference-design-free modeling technique [15], where the surrogate domain is constricted so that it encloses the parameter vectors of high quality as considered by the designer. Such a domain is considerably smaller volume-wise than the traditional domain. Thus, constructing the surrogate therein is significantly cheaper.

The notation utilized in the techniques [13] and [15] is summarized in Fig. 1. Observe that in any performance-driven technique, the modeling process is objective-oriented (i.e., focuses on the space of design objectives  $F$ ), rather than the design space  $X$ .

Let us introduce the notion of design optimality [15] assessed with the use of the performance metric  $U(\mathbf{x}, \mathbf{f})$ , which  $U(\mathbf{x}, \mathbf{f})$  appraises the quality of the vector  $\mathbf{x}$  w.r.t. the vector of design objectives  $\mathbf{f}$ . Consider an exemplary dual-band antenna and the design objectives defined as the operating frequencies  $f_{0,1}$  and  $f_{0,2}$ . If the enhancement of antenna impedance matching over the fractional bandwidths  $B$  centered at both frequencies is of interest, then we may use  $U(\mathbf{x}, \mathbf{f}) = U(\mathbf{x}, [f_{0,1} f_{0,2}]^T) = \max\{S_1(\mathbf{x}, \mathbf{f}), S_2(\mathbf{x}, \mathbf{f})\}$  (i.e., the merit function is defined as the maximum in-band reflection), with  $S_k = \max\{f_{0,k}(1 - \beta/2) \leq f \leq f_{0,k}(1 + \beta/2) : |S_{11}(\mathbf{x}, f)|\}$ ,  $k = 1, 2$ , and  $f$  standing for the frequency.

Symbol	Description	Comments
$\mathbf{x} = [x_1 \dots x_n]^T$	Vector of antenna parameters	Independent antenna dimensions to be tuned in the design process
$X = [\mathbf{l} \mathbf{u}]$	Conventional parameter space	$\mathbf{l} = [l_1 \dots, l_n]^T$ and $\mathbf{u} = [u_1 \dots, u_n]^T$ are lower and upper bounds on parameters, i.e., $l_k \leq x_k \leq u_k$ for $k = 1, \dots, n$
$f_k, k = 1, \dots, N$	Figures of interest	May include operating frequency (or frequencies), bandwidth, substrate permittivity, etc.
$\mathbf{f} = [f_1 \dots f_N]^T$	Objective vector	Aggregates figures of interest pertinent to the antenna structure of interest
$F$	Objective space	Defined by ranges for figures of interest $f_{k,\min} \leq f_k^{(j)} \leq f_{k,\max}$ , $k = 1, \dots, N$ , over which the surrogate is to be valid

Fig. 1. Notation of the nested kriging [13] and observable-based [15] modeling techniques.

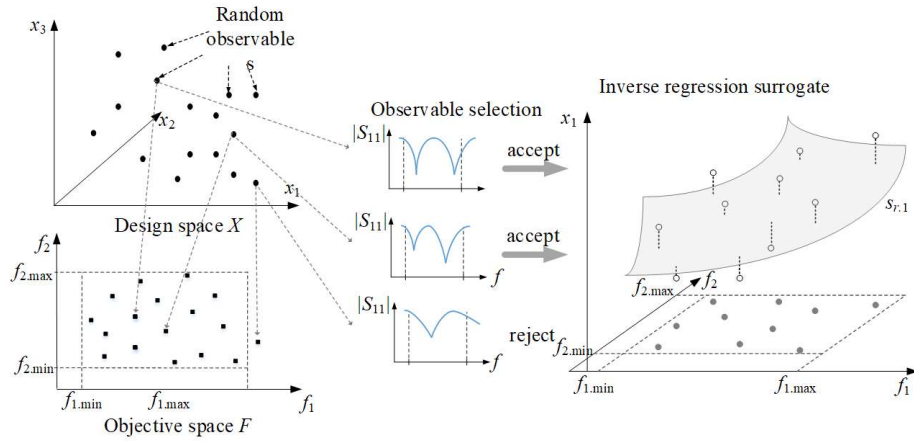


Fig. 2. (left) Observable generation for a dual-band antenna ( $X$ : 3-dimensional,  $F$ : 3-dimensional). (middle) Observable selection: samples of operating frequencies  $\in F$  are kept, other are discarded. (right) Construction of an inverse model  $s_r(\cdot)$  using the observable set  $\{\mathbf{x}_r^{(j)}\}_{j=1,\dots,N_r}$ , for a single component of  $s_{r,j}$ , corresponding to parameter  $x_1$  (shown as gray manifold).

Having defined  $U(\mathbf{x}, \mathbf{f})$ , the following minimization task is solved

$$\mathbf{x}^* = U_F(\mathbf{f}) = \arg \min_{\mathbf{x}} U(\mathbf{x}, \mathbf{f}) \quad (1)$$

where  $\mathbf{x}^*$  refers to the optimal solution. We also define the  $N$ -dimensional manifold in the parameter space  $X$  comprising all the vectors rendered using (1) for all  $\mathbf{f} \in F$ :  $U_F(F) = \{U_F(\mathbf{f}) : \mathbf{f} \in F\}$ . Setting up the surrogate model over the optimum design set suffices for ensuring the model design usability w.r.t. objective space  $F$ . Clearly, it is not possible to accurately identify  $U_F(F)$  because this would require finding optimal solutions of (1) for all  $\mathbf{f} \in F$ . Thus, its location within the design space  $X$  may be only roughly assessed. In the technique of [15], this is established by using random observables. As a consequence, the expenses associated with surrogate construction are low, whereas, the modeling accuracy is maintained at the same level as in the nested kriging [15]. Here, the aim is to improve the cost-efficiency even further by executing the modeling process in the domain of reduced dimensionality.

## 2.2 Domain Definition

In the reference-design-free constrained modeling [15], only a rough identification of  $U_F(F)$  is possible, because the information pertaining to the location of the optimum design manifold encompassed in the observables is not precise. Thus, in [15], an auxiliary inverse regression surrogate is employed for the surrogate domain definition. This model is constructed as follows: over the design space  $X$ , the set of observables  $\mathbf{x}_r^{(j)}$ ,  $j = 1, 2, \dots$ , following a uniform probability distribution is gathered. Next, the respective responses are simulated, and the performance figure vectors  $\mathbf{f}_r^{(j)}$  are extracted therefrom. Next, a selection procedure is carried out: each vector  $\mathbf{f}_r^{(j)}$  is examined whether it belongs to the assumed objective space  $F$  (in such a case, the corresponding observable is accepted) or not (it is discarded). Figure 2 presents a visualization of the selection process for a dual-band antenna example. Generation of the observables is terminated if the assumed number  $N_r$  is collected (typically, between 50 and 100).

We utilize an auxiliary inverse model  $s_r : F \rightarrow X$ , which is built using the pairs:  $\{\mathbf{x}_r^{(j)}, \mathbf{f}_r^{(j)}\}_{j=1, \dots, N_r}$ , i.e., the retained observables and the corresponding performance figures. In general, the observable quality is low, thus, the model  $s_r$  provides only a rough regression of the dataset. So, a simple analytical form is exploited [15]

$$s_r(\mathbf{f}) = \mathbf{s}_r \left( [f_1 \dots f_N]^T \right) = \begin{bmatrix} s_{r,1}(\mathbf{f}) \\ \dots \\ s_{r,n}(\mathbf{f}) \end{bmatrix} = \begin{bmatrix} a_{1,0} + a_{1,1} \exp\left(\sum_{k=1}^N a_{1,k+1} f_k\right) \\ \dots \\ a_{n,0} + a_{n,1} \exp\left(\sum_{k=1}^N a_{n,k+1} f_k\right) \end{bmatrix} \quad (2)$$

Despite featuring a small number of coefficients, the model (2) is sufficiently flexible. Identification of coefficients requires solving the weighted nonlinear regression task

$$\left[ a_{j,0} \ a_{j,1} \ \dots \ a_{j,K+1} \right] = \arg \min_{[b_0 \ b_1 \ \dots \ b_{K+1}]} \sum_{k=1}^{N_r} w_k \left[ s_{r,j}(\mathbf{f}_r^{(k)}) - x_{r,j}^{(k)} \right]^2, \quad j = 1, \dots, n \quad (3)$$

where  $\mathbf{x}_r^{(k)} = [x_{r,1}^{(k)} \ \dots \ x_{r,n}^{(k)}]^T$ , and the multipliers  $w_k$  serve to discriminate between the observables of different qualities. The latter requires defining auxiliary vectors  $\mathbf{p}_r^{(j)} = [p_{r,1}^{(j)} \ \dots \ p_{r,N}^{(j)}]^T$  which are based on the evaluations of the design quality metric, and are derived from EM-evaluated antenna responses. The weights  $w_k$  are defined as  $w_k = [(W - \max\{p_1(\mathbf{x}^{(j)}), \dots, p_N(\mathbf{x}^{(j)})\})/W]^2$ ,  $k = 1, \dots, N_r$ , with  $W = \max\{k = 1, \dots, N_r, j = 1, \dots, N : p_j^{(k)}\}$  being a normalization factor. The weighted regression is employed to ensure that better-quality vectors have a more profound effect on the regression surrogate, which is advantageous because they reside close to the optimum design set. The inverse surrogate for the exemplary dual-band antenna is shown graphically in Fig. 2. Surrogate  $s_r(F)$  gives a rough appraisal of the manifold  $U_F(F)$  of the optimal designs. The domain of the ultimate surrogate, rendering the antenna responses, is to encompass the entire  $U_F(F)$ , so we need to perform its orthogonal extension, as in [15].

First, a set of designs is allocated on  $s_r(F)$  uniformly w.r.t. the objective space  $F$  on a rectangular grid  $F_G \subset F$ . The vector of objectives  $\mathbf{f}_g = [f_{g,1} \ \dots \ f_{g,n}]^T$  resides on the grid, if and only if  $f_{g,k} = f_{k,\min} + (f_{k,\max} - f_{k,\min})m_k/(M - 1)$ ,  $k = 1, \dots, N$ , where  $m_k \in \{0, 1, \dots, M - 1\}$ , and  $M$  is grid density (its value is not critical, we set  $M = 4$  or  $5$ ). The grid  $F_G$  encompasses  $M^N$  vectors in total. Thus, we have the points  $\mathbf{x}_g^{(j)} = s_r(\mathbf{f}_g^{(j)})$ ,  $j = 1, \dots, M^N$ , which render an approximate spatial allocation of the image  $s_r(F)$  of the inverse model.

Symbol	Description	Default value and comments
$N_r$	Number of random observables	Typically set between 50 and 100. The value is not critical, but should be larger for higher-dimensional objective spaces
$p$	Surrogate domain dimensionality	Typically set to $p = 3$ ; the required value can be estimated by based on the analysis of the eigenvalues $\lambda_k$
$N_B$	Number of training data samples for model construction	Depends on required predictive power of the surrogate model. Typical values to ensure relative RMS error of a few percent are between 200 to 500 samples

Fig. 3. Control parameters of the introduced modeling procedure with reduced dimensionality.

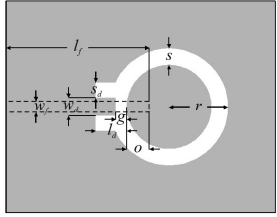
	Substrate	$\epsilon_r$ – operating parameter, $h = 0.76$ mm
	Design parameters <sup>§</sup>	$\mathbf{x} = [l_f \ l_d \ w_d \ r \ s \ s_d \ o \ g]^T$
Other parameters <sup>§</sup>	EM model	$w_r$ – adjusted for 50Ω line impedance CST (~300,000 cells, sim. time 90 s)
Figures of interest	Objective space	Center freq. $f_0$ ; substrate permittivity $\epsilon_r$ $2.5 \text{ GHz} \leq f_0 \leq 6.5 \text{ GHz}$ , $2.0 \leq \epsilon_r \leq 5.0$
Design optimality	Conventional parameter space $X$	Minimum reflection at target operating frequency and substrate permittivity $\mathbf{l} = [22.0 \ 3.5 \ 0.3 \ 6.5 \ 3.0 \ 0.5 \ 3.5 \ 0.2]^T$ , $\mathbf{u} = [27.0 \ 8.0 \ 2.3 \ 16.0 \ 7.0 \ 5.5 \ 6.0 \ 2.3]^T$
What is modelled?		Reflection response $S_{11}$ <sup>§</sup> Dimensions in mm.

Fig. 4. (a) Ring-slot antenna [17], (b) details on antenna structure.

Next, the spectral analysis of the set  $\{\mathbf{x}_g^{(j)}\}_{j=1, \dots, M^N}$ , is carried out so as to find the most important correlations between the coordinates of these designs. We define a covariance matrix  $\mathbf{S}_g = [\sum_{j=1, \dots, M^N} (\mathbf{x}_g^{(j)} - \mathbf{x}_m) (\mathbf{x}_g^{(j)} - \mathbf{x}_m)^T] / (M^N - 1)$ , with  $\mathbf{x}_m = [\sum_{j=1, \dots, M^N} \mathbf{x}_g^{(j)}] / M^N$  being the set's center. The principal components [16] of  $\mathbf{S}_g$  are referred to as  $\mathbf{v}_k$ ,  $k = 1, \dots, n$  (eigenvectors), and  $\lambda_k$ ,  $k = 1, \dots, n$  (eigenvalues; listed in a descending sequence, i.e.,  $\lambda_1 \geq \lambda_2 \geq \dots \geq \lambda_n \geq 0$ ). Typically, only the first few eigenvectors are meaningful. Thus, surrogate domain is delimited using them.

We use the following expansion  $\mathbf{x}_g^{(j)} = \mathbf{x}_m + \sum_{k=1, \dots, n} b_{jk} \mathbf{v}_k$ . We also have the center point:  $\mathbf{x}_c = \mathbf{x}_m + [\mathbf{v}_1 \ \mathbf{v}_2 \ \dots \ \mathbf{v}_n] \mathbf{b}_0$ , where the entries of the vector  $\mathbf{b}_0 = [b_{1,0} \ \dots \ b_{n,0}]^T$  are:  $b_{j,0} = (b_{j,\max} - b_{j,\min})/2$ ,  $j = 1, \dots, n$ , and  $b_{j,\max} = \max\{k : b_{kj}\}$ ,  $b_{j,\min} = \min\{k : b_{kj}\}$ , as well as the eigenvalue vector  $\boldsymbol{\lambda} = [\lambda_{b1} \ \dots \ \lambda_{bn}]^T$ , with  $\lambda_{bj} = 0.5(b_{j,\max} + b_{j,\min})$ . The confined domain of reduced dimensionality, spanned by the vectors  $\mathbf{v}_1$  through  $\mathbf{v}_p$ , is defined as

$$X_p = \left\{ \begin{array}{l} \mathbf{x} = \mathbf{x}_c + \sum_{k=1}^p (2\lambda_k - 1) \lambda_{b_k} \mathbf{v}_k \\ 0 \leq \lambda_k \leq 1, \ k = 1, \dots, p \end{array} \right\} \quad (4)$$

In practice, the eigenvalues are quickly decreasing, so it suffices to exploit  $p$  directions, where  $p$  is much smaller than  $n$  (the design space dimensionality), which is beneficial from the point of view of the training data acquisition.

The control parameters of the developed modeling procedure along with the discussion of their recommended values are presented in Fig. 3. The procedure requires supplying the following input parameters: lower and upper bounds on parameters  $\mathbf{l}$  and  $\mathbf{u}$  delimiting the conventional parameter space  $X$ , as well as the bounds for operational conditions delimiting the space of design objectives  $F$ . Observe that in the presented approach, the final surrogate is built from both the training data set  $\{\mathbf{x}_B^{(j)}\}$  and the observable data  $\{\mathbf{x}_r^{(j)}\}$ . This is to improve the overall modeling accuracy.

### 3 Results

This section demonstrates the performance of the introduced modeling methodology along with its design utility. Benchmarking against state-of-the-art data-driven techniques is provided as well. Figure 4 shows a ring-slot antenna employed as a verification case. Here, the aim is to build surrogate models representing complex reflection responses  $S_{11}$  versus frequency.

The surrogate models have been built using the technique of Section 2. The number of retained observables is set to  $N_r = 50$ , which required generating a total of 106 samples. The reduced dimensionality of the model domain was set to  $p = 3$ . To study the model scalability, the surrogates were rendered for training data sets of sizes  $N_B = 50, 100, 200, 400,$  and  $800$ . The benchmark methods include: (i) kriging (in the standard space  $X$ ); (ii) radial basis function (RBF) (within  $X$ ); (iii) convolutional neural network (CNN) [18] (within  $X$ ); (iv) Ensemble Learning [19] (in the confined domain  $X_S$ ); (v) nested kriging [13] (within  $X_S$ ); the cost of identifying the database designs is 864 EM simulations, (vi) reference-design-free constrained model [15], set up in domain  $X_S$ ; the cost of generating the observables is added to the overall surrogate set up expenses, which is the same as for the method of Section 2. The predictive power of the surrogates is quantified using a relative RMS error, defined as  $\|\mathbf{R}_s(\mathbf{x}) - \mathbf{R}_f(\mathbf{x})\|/\|\mathbf{R}_f(\mathbf{x})\|$ , with  $\mathbf{R}_s$  and  $\mathbf{R}_f$  being the responses predicted by the surrogate and EM analysis. The error is computed using 100 randomly allocated test points.

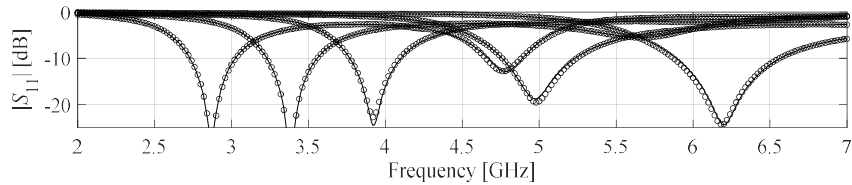


Fig. 5. Reflection responses at the selected test locations: EM model (—), and the introduced constrained surrogate with dimensionality reduction (o). The surrogate built with  $N_B = 400$  data samples.

Table 1. Modeling results and benchmarking for ring-slot antenna

Modeling method		Number of training samples				
		50	100	200	400	800
Kriging	Modeling error	56.9 %	50.8 %	35.8 %	31.5 %	25.6 %
	Model setup cost	50	100	200	400	800
RBF	Modeling error	61.0 %	53.2 %	37.9 %	34.1 %	27.2 %
	Model setup cost	50	100	200	400	800
CNN	Modeling error	67.7 %	58.8 %	34.0 %	22.3 %	13.5 %
	Model setup cost	50	100	200	400	800
Ensemble learning	Modeling error	73.8 %	69.1 %	63.9 %	58.1 %	55.8 %
	Model setup cost	50	100	200	400	800
Nested kriging [13]	Modeling error	19.4 %	12.9 %	7.7 %	5.1 %	3.7 %
	Model setup cost <sup>§</sup>	914	964	1,064	1,264	1,664
Constrained modeling [15]	Modeling error	13.4 %	9.9 %	6.9 %	5.4 %	4.4 %
	Model setup cost <sup>#</sup>	156	206	306	506	906
This work	Modeling error	14.3 %	10.1 %	6.7 %	3.5 %	2.2 %
	Model setup cost <sup>#</sup>	156	206	306	506	906

<sup>§</sup>The cost includes acquisition of the reference designs.

<sup>#</sup>The cost includes generation of random observables, here, 106 simulations in total to yield  $N_r = 50$  accepted samples.

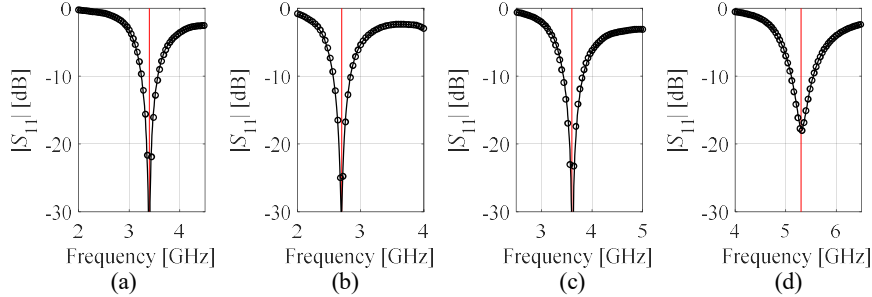


Fig. 6. Optimization using the proposed surrogate: surrogate prediction (o) and EM-evaluated characteristics (—) at the design yielded by optimizing the model. The responses evaluated for  $F = [f_0 \ \varepsilon_r]$  (frequency in GHz): (a)  $F = [3.4 \ 3.6]$ , (b)  $F = [2.7 \ 4.3]$ , (c)  $F = [3.6 \ 2.2]$ , (d)  $F = [5.3 \ 4.3]$ . The intended operational frequency is shown with vertical line.

Table 1 provides numerical results, and Fig. 5 shows the antenna responses for the selected test locations. The accuracy of our model is superior to all models built in the parameter space  $X$ , and also to nested kriging, which is mainly a result of dimensionality reduction and volume-wise confinement. Cost-efficiency of our method is better than that of nested kriging because no reference designs are required, thus the overall numbers of EM analyses is reduced by 80 percent for  $N_B = 50$ . For  $N_B = 800$ , the reduction is 45 percent. The efficiency of our method is identical to that of the procedure of [19].

Figure 6 shows the results of applying the proposed surrogate (constructed using 800 training samples) to optimize a ring-slot antenna for a variety of operating frequencies and substrate permittivity  $\varepsilon_r$ . It can be observed that satisfactory designs are obtained for all assumed targets, which corroborates design utility of the models.

## 4 Conclusion

This article proposed a novel procedure for cost-efficient surrogate modeling of antenna structures. Our technique capitalizes on the performance-driven paradigm with the model domain established in the region containing high-quality designs. A supplementary dimensionality reduction is applied by spanning the domain along the most relevant directions that account for spatial orientation of the initially established region of interest. These mechanisms lead to a dramatic increase in the surrogate model predictive power without compromising its design usefulness. Both features have been conclusively corroborated through extensive benchmarking and application case studies.

## Acknowledgement

The authors would like to thank Dassault Systemes, France, for making CST Microwave Studio available. This work is partially supported by the Icelandic Centre for Research (RANNIS) Grant 217771 and by National Science Centre of Poland Grant 2018/31/B/ST7/02369.

## References

1. Wang, Y., Zhang, J., Peng, F., Wu, S.: A glasses frame antenna for the applications in internet of things. *IEEE Internet of Things J.*, **6**(5), pp. 8911–8918 (2019)
2. Tu, S., Cheng, Q.S., Zhang, Y., Bandler, J.W., Nikolova, N.K. Space mapping optimization of handset antennas exploiting thin-wire models. *IEEE Trans. Ant. Propag.*, **61**(7), pp. 3797–3807 (2013)
3. Kolda, T.G., Lewis, R.M., Torczon, V.: Optimization by direct search: New perspectives on some classical and modern methods. *SIAM Rev.*, **45**, pp. 385–482 (2003)
4. Tang, M., Chen, X., Li, M., Ziolkowski, R. W.: Particle swarm optimized, 3-D-Printed, wideband, compact hemispherical antenna. *IEEE Ant. Wireless Propag. Lett.*, **17**(11), pp. 2031–2035 (2018)
5. Hassan, E., Noreland, D., Augustine, R., Wadbro, E., Berggren, M.: Topology optimization of planar antennas for wideband near-field coupling. *IEEE Trans. Ant. Prop.*, **63**(9), pp. 4208–4213 (2015)
6. Koziel, S., Pietrenko-Dabrowska, A.: Reduced-cost electromagnetic-driven optimization of antenna structures by means of trust-region gradient-search with sparse Jacobian updates. *IET Microwaves Ant. Prop.*, **13**(10), pp. 1646–1652 (2019)
7. Simpson, T.W., Pelplinski, J.D., Koch, P.N., Allen, J.K.: Metamodels for computer-based engineering design: Survey and recommendations., *Eng. Comput.* **17**, pp. 129–150 (2001)
8. Cervantes-González, J. C., Rayas-Sánchez, J. E., López, C. A., Camacho-Pérez, J. R., Brito-Brito, Z., Chávez-Hurtado, J. L.: Space mapping optimization of handset antennas considering EM effects of mobile phone components and human body. *Int. J. RF Microwave CAE*, vol. 26, no. 2, pp. 121–128 (2016)
9. Forrester, A.I.J., Keane, A.J.: Recent advances in surrogate-based optimization. *Prog. Aerospace Sci.*, **45**, pp. 50–79 (2009).
10. Kabir, H., Wang, Y., Yu, M., Zhang, Q.J.: Neural network inverse modeling and applications to microwave filter design. *IEEE Trans. Microwave Theory Tech.*, **56**(4), pp. 867–879 (2008)
11. Melgarejo, J.C., Ossorio, J., Cogollos, S., Guglielmi, M., Boria, V.E., Bandler, J.W.: On space mapping techniques for microwave filter tuning. *IEEE Trans. Microw. Theory Tech.*, **67**(12), 4860–4870 (2019)
12. Koziel, S.: Fast simulation-driven antenna design using response-feature surrogates. *Int. J. RF & Micr. CAE*, **25**(5), pp. 394–402 (2015)
13. Koziel, S., Pietrenko-Dabrowska, A.: Performance-based nested surrogate modeling of antenna input characteristics. *IEEE Trans. Ant. Prop.*, **67**(5), pp. 2904–2912 (2019)
14. Koziel, S., Pietrenko-Dabrowska, A.: Performance-driven surrogate modeling of high-frequency structures. Springer, New York (2020)
15. Koziel, S., Pietrenko-Dabrowska, A.: Knowledge-based performance-driven modeling of antenna structures. *Knowledge Based Systems*, **237**, paper no. 107698 (2022)
16. Jolliffe, I.T.: *Principal component analysis*, 2nd ed., Springer, New York (2002).
17. Koziel, S., Pietrenko-Dabrowska, A.: Design-oriented modeling of antenna structures by means of two-level kriging with explicit dimensionality reduction. *AEU Int. J. Electronics Comm.*, **127**, pp. 1–12 (2020)
18. Mahouti, P.: Application of artificial intelligence algorithms on modeling of reflection phase characteristics of a nonuniform reflectarray element. *Int J Numer Model*, **33** (2020)
19. Zhang, Y., Xu, X.: Solubility predictions through LSBoost for supercritical carbon dioxide in ionic liquids. *New J. Chem.*, **44**, pp. 20544–20567 (2020)